Mechanical improvement of P(VDF-TrFE) /nickel nanowires conductive nanocomposites: Influence of particles aspect ratio

Antoine Lonjon *, Philippe Demont, Eric Dantras, Colette Lacabanne

Physique des polymères, Institut Carnot CIRIMAT Université Paul Sabatier, 118 route de Narbonne, 31062 Toulouse Cedex 9, France

Keywords:
Shear modulus;
Nanowires;
Nanocomposites;
Conductive nanocomposites;
Crystallinity

A B S T R A C T

Nickel nanowires with high aspect ratio (250) were elaborated and incorporated into poly(vinylidene difluoride-trifluoroethylene) up to 30 vol% via solvent mixing way. These nanocomposites are characterized by a conductive behavior with a high electrical conductivity value (10^2 S m^{-1}) above a very low percolation threshold (0.75 vol% of metallic nanowires). The introduction of nanowires strongly depressed the matrix crystallinity. Static and dynamic mechanical analysis have been realized at low nanowire volume fraction (<10 vol%). Below 5 vol% of nanowires, nanocomposites remain ductile. The dynamic mechanical properties are related to the volume fraction of nanowires. A strong increase of the viscoelastic contribution related to the increase of the percentage of amorphous phase is observed. The major effect is the increase of the rubbery modulus. The highest increase of 300% is obtained for only 5 vol% of nanowires; it represents an original mechanical result for low filled composites. The dependence versus nanowire content has been described by adapting the Halpin–Tsai model to high aspect ratio filler. Metallic nanowires create additional entanglements that are randomly distributed in the rubbery polymeric matrix. With their low percolation threshold, metallic nanowires based nanocomposites constitute a new class of multifunctional materials with a high conductivity associated with a ductile polymer matrix characterized by a high rubbery modulus.

1. Introduction

In the past decades, the objective of conductive polymer composites was focused on the ability to conduct the electrical current and to obtain the maximum of conductivity value. These composites were realized with conventional conductive fillers like carbon black [1] or metallic particles [2,3]. The conductive characteristic was obtained to the detriment of final weight and mechanical properties. Conductive polymer composites maintaining the structural properties of the matrix are emerging as a new class of multifunctional materials. The mechanical properties conservation is directly linked to the conductive filler ratio, filler morphology, filler size and filler dispersion quality.

Conductive nanoparticles with specific geometries allow low percolation threshold [4–7]. Carbon nanotubes possess a high aspect ratio ($\xi = L/D \sim 1\,000$). This characteristic permits to observe a percolation threshold at very low filler content ($\phi < 1$ vol%) [8]. The highest value of electrical conductivity reaches 10^{-1} S m^{-1} above the percolation threshold [8]. New kind of conductive metallic nanoparticles like nanowires, with high aspect ratio ($\xi \approx 250$) have attracted considerable attention. Nickel nanowires could be produced in great quantity by electrodeposition in anodic aluminium oxide. Metallic filler has preserved the specific properties of the bulk as mechanical resistance [9–11], stiffness [12], electrical conductivity [13,14], and magnetic susceptibility [15]. In recent works nickel nanowires have been incorporated to obtain magnetic elastomers composites [16], EMI shielding [17] or conductive nanowires nanocomposites [7,18]. In this last case [7], the percolation threshold was obtained about 1 vol% and the level of electrical conductivity reaches 100 S m^{-1}. These specific properties show that nanowires nanocomposites are well suited candidates for the formulation of multifunctional polymers.

In this paper, we will focus on mechanical properties of conductive polymer nanocomposites [7]. The influence of nickel nanowires volume fraction according to shear and tensile stress has been studied. Physical structure of the nanocomposite has been determined using differential scanning calorimetry; mechanical behavior has been analysed from stress–strain curves and from dynamic mechanical analysis (DMA).

2. Experimental section

2.1. Materials and sample preparation

Nickel nanowires (NW) were synthesized by electrochemical deposition in an anodic aluminium oxide (AAO) porous template. The electrolyte used for nickel deposition was a standard Watts bath with an accurate pH value of 4. Direct current (DC) electrodeposition was carried out at room temperature using a Nickel wire as anode with 1.0 mm in

* Corresponding author.
E-mail address: lonjon@cict.fr (A. Lonjon).

0022-3093/$ – see front matter
doi:10.1016/j.jnoncrysol.2011.09.019

diameter. A porous (AAO) membrane of 200 nm diameter and 50 μm thickness was supplied by Whatman. One side of the AAO membrane was coated with a 35 nm thickness silver layer by using sputtering technique as cathode for electrodeposition. Nickel NWs growing was controlled by the time deposition and the direct current intensity using a Keithley 2420 source meter. The AAO membrane was dissolved in NaOH 6 M for 30 min, releasing Ni NWs from the template. Then, Ni NWs were washed with distilled water and filtrated. A following sonication leaded to a very good dispersion of NWs in water. The NWs size is equal to the AAO pore one, 200 nm in diameter with length 50 μm. Oxide layer was observed on Ni NWs which are responsible for the decrease of NW conductivity. A chemical method for removing the oxide layer was used. The NWs were poured in 0.25 M solution of H_2SO_4 at 60 °C and a stirring at 400 rpm for 5 min. The treated nanowires were filtered, rinsed with water and stored in acetone.

Poly(vinylidene fluoride–trifluoroethylene) P(VDF-TrFE) (70/30) mol% copolymer was supplied by Piezotech S.A. (Hésingue, France). Melting temperature of 150 °C was determined by differential scanning calorimetry and the density was about 1.8 g cm^{-3}.

The nanocomposites were prepared by using solvent casting method. P(VDF-TrFE) was dissolved into acetone. The nanowires acetone suspension was poured into the polymer solution and the mixture was submitted to 5 s short pulse of sonication, corresponding to a dissipated power of 25 W. Sonication parameters were optimized by the observation of Ni NWs dispersion using Scanning Electron Microscopy (SEM) [7]. The solvent was evaporated using a magnetic stirrer at 80 °C for 1 h. Pellets of randomly dispersed Ni NWs in P(VDF-TrFE) matrix were obtained. Sample geometry is a parallelepiped with 40 mm length, 10 mm width and 1 mm in thickness. No residue of solvent was found in the thermogravimetric analysis, indicating a complete removal of acetone from samples. Ni NWs/P(VDF-TrFE) nanocomposites were elaborated with a volume fraction varying from 0 to 30 vol%. The nanocomposites prepared according this method [7] exhibit an high conductive behavior near 10^2 S m^{-1} above the percolation (0.75 vol%).

2.2. Electron microscopy

The morphology of the nickel nanowires was examined by scanning electron microscope using a JEOL JSM 6700F equipped with a field emission gun (SEM-FEG). Nanocomposite samples were fractured at the liquid nitrogen temperature for observation by SEM.

2.3. Differential scanning calorimetry

Crystallization and melting phenomena of the nanocomposites were investigated using a TA Instruments 2920 differential scanning calorimeter (DSC). Before the heating and cooling runs, the samples were melted at 200 °C and maintained at this temperature for 5 min in order to erase the thermal history. The samples were then cooled from 200 to 20 °C at a rate of 10 °C min^{-1} and then heated from 20 to 200 °Cat 10 °C min^{-1}. All the DSC measurements were performed under helium atmosphere. The transition temperatures were taken as the peak maximum or minimum in the DSC curves. The degree of crystallinity of the P(VDF-TrFE) composites was calculated according to the weight fraction of polymer using the calculated value of enthalpy corresponding to a theoretical 100% crystalline P(VDF-TrFE) (70/30) copolymer, $\Delta H_{0m} = 91.45$ J g^{-1} [19].

2.4. Mechanical analysis

Stress–strain study was performed on a Hounsfield tensile tension machine at 25 °C. The extensional speed was set to 0.5 mm/min and each sample was pulled beyond the elastic range. The dynamic mechanical study was performed by dynamic mechanical analysis (DMA) on an ARES of TA Instruments. Tests were carried out in torsion rectangular mode over the linear elasticity range (10^{-1}% strain at angular frequency of 1 rad s^{-1}). This technique allows us to access to the complex shear modulus $G^*(\omega,T)$.

$$G^*(\omega,T) = G'(\omega,T) + iG''(\omega,T) \tag{1}$$

Since nanocomposites are isotropic, the shear modulus G and the elongation modulus E are linked through the ν Poisson's coefficient.

$$G = \frac{E}{2(1+\nu)} \tag{2}$$

The Hashin–Shtrikman (HS) [20] model predicts the evolution of the shear modulus of an heterogeneous material like composite with the ratio of a rigid phase (filler) homogeneously dispersed in a soft phase (matrix) with arbitrary geometry. As for the Reuss and Voigt model, this model introduces upper and lower bounds; upper bound, when the reference modulus is the rigid material and lower bound for the soft material as reference. Often used for particulate composites, this model, is tighter than Reuss and Voigt models.

$$G_c^{up} = G_f + \frac{1-\phi}{\frac{1}{G_m - G_f} + \frac{6\phi(K_f + 2G_f)}{5G_f(3K_f + 4G_f)}} \tag{3}$$

$$G_c^{low} = G_m + \frac{\phi}{\frac{1}{G_f - G_m} + \frac{6(1-\phi)(K_m + 2G_m)}{5G_m(3K_m + 4G_m)}} \tag{4}$$

ϕ is the volume fraction of filler; K_m and G_m are the bulk and the shear moduli of the matrix; K_f and G_f are the bulk and the shear moduli of the filler.

The lower bound fits perfectly hard spherical particles dispersed in soft matrix and corresponds to the Kerner model [21]. This model have demonstrated its accuracy in spherical silica dispersed in polyamide matrix nanocomposites [22].

$$G_c = G_m \frac{\frac{\phi G_f}{(7-5\upsilon_m)G_m + (8-10\upsilon_m)G_f} + \frac{(1-\phi)}{15(1-\upsilon_m)}}{\frac{\phi G_m}{(7-5\upsilon_m)G_m + (8-10\upsilon_m)G_f} + \frac{(1-\phi)}{15(1-\upsilon_m)}} \tag{5}$$

Where ϕ is the volume fraction of fillers, G_m and υ_m are the shear modulus and the Poison's ratio of the matrix; G_f is the shear modulus of the filler.

The HS model does not take into account the aspect ratio of particles. The P(VDF-TrFE)/Ni NWs behavior is in the bound of HS model, confirming the good dispersion of nanowires.

The Halpin–Tsai (HT model) [23,24] was widely used to predict the behavior of fibrous composites. The fibers are aligned and oriented. HT has included the shape of the filler phase in the model:

$$M_c = M_m \frac{1 + \xi\eta\phi}{1 - \eta\phi} \tag{6}$$

$$\eta = \frac{\frac{M_f}{M_m} - 1}{\frac{M_f}{M_m} + \xi} \tag{7}$$

The Halpin–Tsai equation could be rewritten as:

$$M_c = M_m \frac{M_f + \xi[(1-\phi)M_m + \phi M_f]}{[(1-\phi)M_f + \phi M_m + \xi M_m]} \tag{8}$$

Where ϕ is the volume fraction of fibers, M_f is the fiber modulus, M_m is the matrix modulus. The parameter ξ is the shape factor, reinforcement factor or contiguity factor [25], and contains the aspect

ratio of particles. When ξ is close to 0, the equation fits the lower bound of Reuss model and when the aspect ratio tends towards infinite the equation fits the upper bound of Voigt model. ξ is dependent on stress direction. For a solicitation parallel to the fiber orientation $\xi = 2(L/d)$ and for a transverse solicitation $\xi = 2$. The resulting moduli arec $M_{\parallel}$ and $M_{\perp}$. This HT model will be used for describing the evolution of the rubbery modulus of nanocomposites as a function of NW content.

3. Results

Fig. 1 shows the SEM image of the nanocomposite for 4 vol% of Ni NWs. The individual NWs are clearly observed because NWs have no affinity in acetone and keep their homogeneous dispersion in the copolymer. In order to obtain hot melt nanocomposite films, a temperature and pressure protocol is necessary. This protocol induces a weak orientation of the nanowires.

3.1. Crystallinity

As P(VDF-TrFE) 70–30 is a semicrystalline polymer, it is necessary to measure the influence of nanowires on the matrix crystallinity since it induces an evolution of the final mechanical properties of composites. The influence of Ni NWs on the crystallization of P(VDF-TrFE) is illustrated in Fig. 2. The crystallinity ratio χ_c decreases linearly as a function of the Ni NWs volume fraction. This fact is coherent with experimental results observed with gold NWs in P(VDF-TrFE) [14]. A similar analysis is reported with Polypropylene filled with layered double hydroxides [26]. The presence of metal filler promotes, in nanocomposites, a less ordered crystalline phase than in pure P(VDF-TrFE) copolymer. Nickel NWs as gold NWs have the same geometry due to the elaboration process. Only metal composition was changed and a similar effect was observed on crystallinity. These results confirm the influence of NWs' aspect ratio on crystallinity decrease. For conductive nanocomposites with low NWs content ($Ø$<5 vol%) the decrease observed was maintained in a range of 90% of the pure P(VDF-TrFE)crystallinity value.

3.2. Yield behavior

The stress–strain studies of the P(VDF-TrFE)/Ni NWs nanocomposites characterized the final mechanical behavior of these composites under longitudinal traction. The stress/strain curves obtained are shown in Fig. 3. Experiments were carried out at 25 °C and described the stiffness and plasticity of nanocomposites for 1, 3, 4 and 5 vol% of nickel nanowires. We observe an increase of the plasticity threshold (σ_{max} with the volume fraction. The highest value obtained for 5 vol% of nanowires

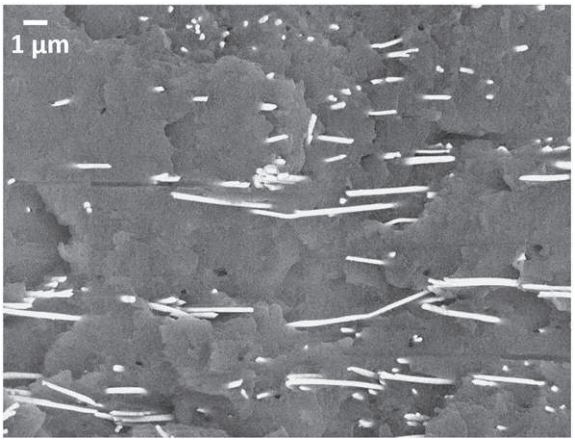

Fig. 1. SEM picture of P(VDF-TrFE) Nickel nanowires nanocomposites for 4 vol %.

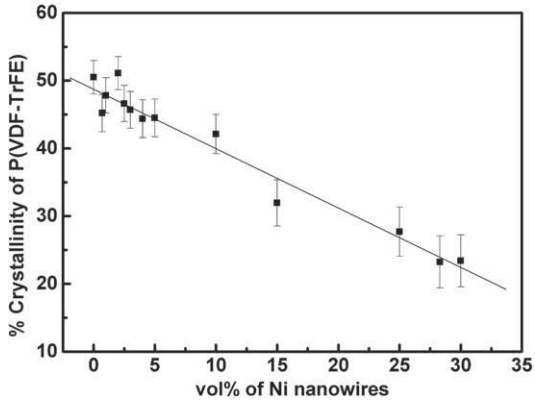

Fig. 2. Crystallinity ratio χ_c of P(VDF-TrFE) matrix as a function of Ni nanowires volume fraction. The line corresponds to the best fit.

exhibits an increase of about 75% from the pristine polymer rupture stress. In parallel, we note a decrease of the strain at break with the increase of nanowires volume fraction. This behavior was observed in classical filled polymer composites with micro and nanoparticles. However, the enhancement measured with nanowires is obtained for very low rate in comparison with spherical particles. Such a strong dependence of the modulus with the particles aspect ratio was observed with glass fibers in PPS matrix [27].

The P(VDF-TrFE)/Ni NWs nanocomposites filled at 5 vol% reaches a brittle behavior while all the samples filled with a lower content of nanowires keep a ductile behavior. These results underline the necessity for conductive nanocomposites to be filled with a nanowires volume fraction below 5 vol% to maintain the ultimate mechanical properties of the polymer matrix.

3.3. Dynamic mechanical relaxation

The real part of the modulus, G'(T) , and the imaginary part G"(T) were measured at $\omega = 1$ rad s^{-1} for samples filled with different Ni nanowires ratio. They are reported in Figs. 4 and 5 respectively. The temperature range was −135 °C to 100 °C with a heating rate of 3 °C/min. We focused the dynamical mechanical study on the β and α relaxation modes associated with the existence of two amorphous phases [28]. The β relaxation ($T_\beta = -33$ °C) corresponds to the free amorphous phase, the α mode ($T_\alpha = 7$ °C) is the response of the constrained amorphous phase [29].

Fig. 6 shows the evolution of G' as function of the NWs volume fraction for the vitreous plateau and the rubbery plateau. The composite modulus shown in Fig. 6 of nanocomposites and pure P(VDF-TrFE) was studied at T_β −50 °C and T_β +50 °C i.e. on the vitreous

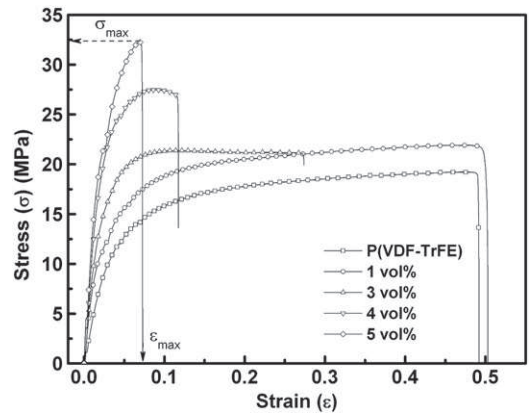

Fig. 3. Stress (σ) versus strain (ε) curves of P(VDF-TrFE)/Ni nanowires composites for volume fractions from 0 vol% to 5 vol%.

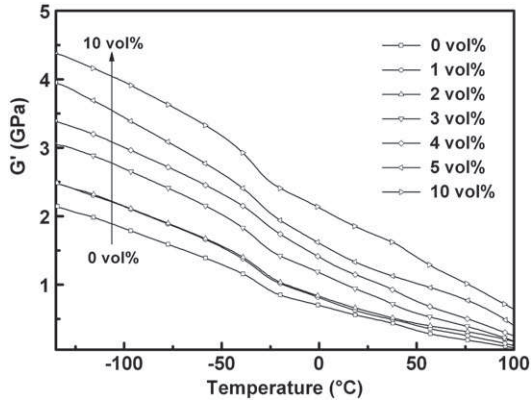

Fig. 4. Storage shear modulus G' versus temperature for P(VDF-TrFE)/Ni nanowires from 0 vol% to 10 vol%.

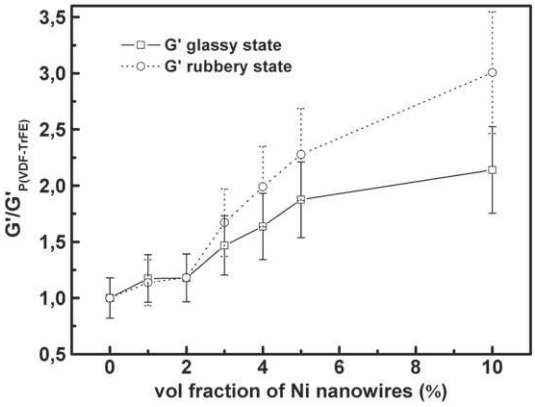

Fig. 6. Storage shear modulus G' of nanocomposites measured on glassy plateau (T_β −50 °C) and on rubbery plateau (T_β + 50 °C) versus the NWs volume fraction (vol%). G' is normalized to the G' of the P(VDF-TrFE) matrix.

and on the rubbery plateau respectively. The effect of NWs is more important on the rubbery plateau.

The G'_c values of nanocomposites were studied as function of the NWs volume fraction and normalized to the G'_m of the P(VDF-TrFE) matrix (Fig. 7). The values of G'_c and G'_m were taken on the rubbery plateau at 25 °C. The introduction of nanowires induces a large increase of the G'_c.

4. Discussion

The dissipative part of the modulus (Fig. 5) was observed as function of the NWs volume fraction. The influence of NWs on the β and α relaxations associated with amorphous phases was studied. The NWs do not modify meaningfully the position in temperature of mechanical relaxations but we observe a slight increasing in the intensity of the mechanical energy loss peaks with the volume fraction of NWs. This evolution corroborates the increasing of amorphous phases inherent with the decrease about 10% of crystallinity for these low rates of filling. Such a G'' evolution was also observed for quenched P(VDF-TrFE) samples [30].

A wide effect of NWs on rubbery plateau was also observed in different kind of composites [31–34]. The nanowires induce a restriction on molecular mobility near the interface between organic and inorganic phases [32,33]. The stiffening associated with the filler is more pronounced on the rubbery plateau [32–34] since there is weaker physical interactions than in the vitreous plateau. In the rubbery state of nanocomposites, NWs plays the role of additional entanglements for polymeric chains.

The phenomenon of G'_c increases with nanowires can be compared to mixing homogenization models. There are many mechanical models

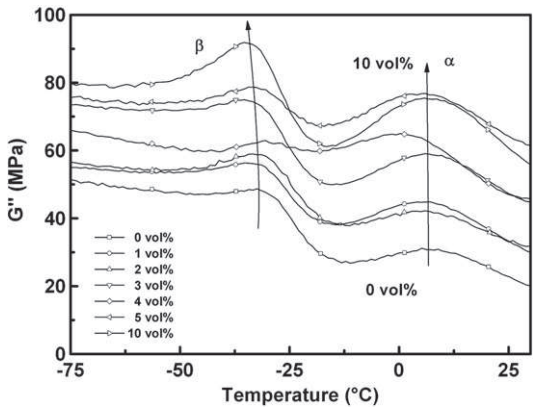

Fig. 5. Dissipative shear modulus G'' of the mechanical β and α relaxations versus temperature for P(VDF-TrFE)/Ni nanowires from 0 vol% to 10 vol%.

based on homogeneous systems with particles dispersed. The first bounding models of Voigt and Reuss were based on finding upper and lower bound for the composite modulus. In our case, the stiffness of the matrix and the NWs are largely different (ratio ~1000). The upper and lower bounds are quite far apart. These models describe a very large domain and do not provide the composite behavior with a quite accuracy.

In order to compare our results to Halpin–Tsai model, we consider that nanowires are homogeneously dispersed in all direction providing a "quasi-isotropic" material. The nanowires size is weak enough in comparison of physical properties measured. In three dimensions we could make an approximation for composites with randomly oriented fibers. Van Es [35] simulated a multitude of rotation around even axis of the modulus of a sheet containing fibers randomly oriented in the plane of the sheet. The calculation shows that modulus converge to an approximation:

$$E_{\text{random 3D fiber}} \cong 0.184\, E_{\parallel} + 0.816 E_{\perp} \tag{9}$$

The properties of randomly oriented composites were intermediate to those longitudinally oriented and transversely oriented composites [36]. Our results were compared to the Halpin–Tsai modified model (9).

The Halpin–Tsai modified model could be converted for shear modulus and was compared to nanocomposites behavior at 25 °C. Our composites filled with spherical nickel microparticles and nanoparticles fit

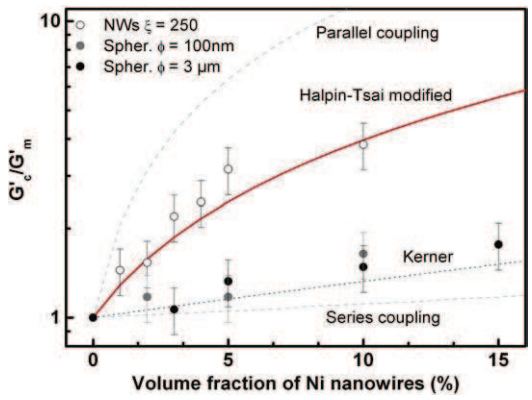

Fig. 7. Storage shear modulus G'_c of nanocomposites values normalized to the G'_m of the P(VDF-TrFE) matrix, versus the nickel volume fraction and particle size : (○) Ni NWs, (●) 100 nm, (●) 3 µm and. Red line corresponds to the Halpin–Tsai modified equation calculated for an aspect ratio ξ = 250. The Kerner model fits the spherical particles for the various sizes.

with accuracy the Kerner's model corresponding to spherical particles and corresponding to Goyal results for micro and nano-spheres composites [37]. The deviation to upper bound of NWs nanocomposites confirms the preponderant effect of filler geometric factor (aspect ratio) on mechanical properties and was also observed with nickel nanowires in PDMS [38]. The Halpin–Tsai modified model is very close to our results for an aspect ratio of 250 introduced in the geometric factor ξ. These results show that Halpin–Tsai model modified by Van Es is well adapted to describe the mechanical behavior of nanowires composites. This model is particularly interesting to link mechanical behavior to particles with an aspect ratio. In our case the increase of modulus is very high for low fraction of particles. The magnification of the effect is due to the high aspect ratio effect previously observed with carbon nano fibres in rubbery matrices [39]. The nanowires induce a restriction in segmental motion in the interface between organic and inorganic phases [32,33]. This observation was confirmed with larger effect observed on rubbery plateau [32–34]. The mixing homogenization models are in good agreement with our results and confirm the homogeneous randomly dispersion of nickel nanowires previously observed by SEM [7] and in Fig. 1. Of course, all these observations are checked at low volume fraction to preserve the homogeneous dispersion and non-interaction between particles.

5. Conclusion

The conservation of mechanical behavior of P(VDF-TrFE)/nickel nanowires is crucial for the elaboration of conductive nanocomposites and future applications. These high conductive nanocomposites tend to preserve mechanical properties of the polymer matrix with low filler content. Stress–strain curves have shown the effect of nanowires on the value of ultimate stress before break (σ_{max}) and (ε_{max}). This effect was obtained for small amount of nanowires (Ø<5 vol%). 5 vol% seems to be the limit to maintain the mechanical properties of P(VDF-TrFE). Nanocomposites exhibit a large improvement of shear modulus (×300). As far as we know, it is an original result at these low filler rates. Above this value a fragile behavior begins. This limit is largely higher than the 1 vol% of NWs necessary to obtain percolation threshold. The nanocomposites filled with a volume fraction of NWs comprise between 1 and 5 vol% keep the mechanical properties of polymeric matrix and exhibit the electrical conductivity of conductive composites. The dynamic study brings more information on relaxations associated to glassy transition and shows an increasing of amorphous phase response. The nanowires filler induce a shear modulus reinforcement different from spherical particles for same material. These results highlight the preponderant influence of high aspect ratio particles on shear modulus increasing. The Halpin–Tsai equations very used for carbon fibrous dispersed in polymeric matrix are particularly adapted to describe mechanical behavior of nanocomposites filled with 1D high aspect ratio nanoparticles like metallic nanowires. The Halpin–Tsai adapted model permits to link the mechanical behavior to the aspect ratio of randomly dispersed nanowires that plays the role of entanglements in the rubbery polymeric matrix. This concept of nanocomposites poorly filled suggests perspectives to obtain multifunctional materials like conductive coatings or structural conductive nanocomposites.

Appendix A. Supplementary data

Supplementary data to this article can be found online at doi:10.1016/j.jnoncrysol.2011.09.019.

References

[1] A.I. Medalia, Rubber Chemistry and Technology 59 (1986) 432.
[2] Y.P. Mamunya, V.V. Davydenko, P. Pissis, E. Lebedev, Eur. Polym. J. 38 (2002) 1887.
[3] M. Karttunen, P. Ruuskanen, V. Pitkanen, W.M. Albers, J. Electron. Mater. 37 (2008) 951.
[4] S. Barrau, P. Demont, A. Peigney, C. Laurent, C. Lacabanne, Macromolecules 36 (2003) 5187.
[5] J.K.W. Sandler, J.E. Kirk, I.A. Kinloch, M.S.P. Shaffer, A.H. Windle, Polymer 44 (2003) 5893.
[6] B. Lin, G.A. Gelves, J.A. Haber, P. Pötschke, U. Sundararaj, Macromol. Mater. Eng. 293 (2008) 631.
[7] A. Lonjon, L. Laffont, P. Demont, Dantras, C. Lacabanne, J. Phys. Chem. C 113 (2009) 12002.
[8] W. Bauhofer, J.Z. Kovacs, Compos. Sci. Technol. 69 (2009) 1486.
[9] H.S. Park, K. Gall, J.A. Zimmerman, Phys. Rev. Lett. 95 (2005) 255504.
[10] Y. Ding, P. Zhang, Z. Long, Y. Jiang, J. Yin, F. Xu, Y. Zuo, J. Alloys Compd. 474 (2008) 223.
[11] B. Wu, A. Heidelberg, J.J. Boland, Nat. Mater. 4 (2005) 525.
[12] S. Miura, M. Kiguchi, K. Murakoshi, Surf. Sci. 601 (2007) 287.
[13] Y.G. Sun, Y.D. Yin, B.T. Mayers, T. Herricks, Y.N. Xia, Chem. Mater. 14 (2002) 4736.
[14] A. Lonjon, L. Laffont, P. Demont, Dantras, C. Lacabanne, J. Phys. D: Appl. Phys. 43 (2010) 345401.
[15] J.X. Xu, X.M. Huang, G.Z. Xie, Y.H. Fang, D.Z. Liu, Mater. Lett. 59 (2005) 981.
[16] K. Keshoju, L. Sun, J. Appl. Phys. 105 (2009) 023515.
[17] X. Shui, D.D.L. Chung, J. Mater. Sci. 35 (2000) 1773.
[18] Y. Tao, Y. Xia, H. Wang, F. Gong, H. Wu, G. Tao, IEEE Trans. Adv. Packag. 32 (2009) 589.
[19] J. Clements, G.R. Davies, I.M. Ward, Polymer 33 (1992) 1623.
[20] Z. Hashin, S. Shtrikman, J. Mech. Phys. Solids 11 (1963) 127.
[21] E.H. Kerner, Proc. Phys. Soc. London B 69 (1956) 808.
[22] E. Reynaud, T. Jouen, C. Gauthier, G. Vigier, J. Varlet, Polymer 42 (2001) 8759.
[23] J.C. Halpin, J.L. Kardos, J. Appl. Phys. 43 (1972) 2235.
[24] J.C. Halpin, J.L. Kardos, Polym. Eng. Sci. 16 (1976) 344.
[25] R.H. Boyd, Polym. Eng. Sci. 19 (1979) 1010.
[26] P.J. Purohit, J.E. Huacuja-Sanchez, D.Y. Wang, F. Emmerling, A. Thunemann, G. Heinrich, A. Schonhals, Macromolecules 44 (2011) 4342.
[27] T.H. Lee, F.Y. Boey, N.L. Loh, Compos. Sci. Technol. 49 (1993) 217.
[28] N. Koizumi, J. Hagino, Y. Murata, Ferroelectrics 32 (1981) 141.
[29] N. Koizumi, N. Haikawa, H. Habuka, Ferroelectrics 57 (1984) 99.
[30] Y. Murata, N. Koizumi, Polym. J. 17 (1985) 385.
[31] J.F. Capsal, C. Pousserot, E. Dantras, J. Dandurand, C. Lacabanne, Polymer 51 (2010) 5207.
[32] P.B. Messersmith, E.P. Giannelis, Chem. Mater. 6 (1994) 1719.
[33] J. Sandler, P. Werner, M.S.P. Shaffer, V. Demchuk, V. Altstadt, A.H. Windle, Composites Part A 33 (2002) 1033.
[34] F. Dalmas, J.Y. Cavaillé, C. Gauthier, L. Chazeau, R. Dendievel, Compos. Sci. Technol. 67 (2007) 829.
[35] Van Es M. Delft University of Technology : PhD Thesis (2001).
[36] J. Kuruvilla, T. Sabu, C. Pavithran, J. Reinf. Plast. Compos. 12 (February 1993) 139.
[37] R.K. Goyal, A.N. Tiwarib, Y.S. Negi, Mater. Sci. Eng., A 491 (2008) 230.
[38] H. Denver, T. Heiman, E. Martin, A. Gupta, D.A. Borca-Tasciuc, J. Appl. Phys. 106 (2009) 064909.
[39] C. Gauthier, L. Chazeau, T. Prasse, J.Y. Cavaille, Compos. Sci. Technol. 65 (2005) 335.